Supplementary Information

Novel sigma 1-antagonists with *cis*-(+)-normetazocine scaffold: synthesis, molecular modeling, and antinociceptive effect

Giuliana Costanzo,[1] Giuseppe Cosentino,[1] Margherita Grasso,[2] Vincenzo Patamia,[1] Sara Zuccalà,[1] Alessandro Coco,[1] Elisabetta Novello,[3] Mahmoud Al-Khrasani,[4] Raffaele Morrone,[5] Giovanni Mario Pitari,[3] Emanuele Amata,[1] Agostino Marrazzo,[1] Antonio Rescifina,[1] Lorella Pasquinucci[1]‡*and Carmela Parenti.[1]‡

[1]Department of Drug and Health Sciences, University of Catania, Viale A. Doria 6, 95125 Catania, Italy.

[2]Oasi Research Institute - IRCCS, Troina, Italy.

[3] Vera Salus Ricerca S.r.l., Via Sigmund Freud 62/B, 96100 Siracusa, Italy.

[4] Department of Pharmacology and Pharmacotherapy, Faculty of Medicine, Semmelweis University, Nagyvárad tér 4, H-1445 Budapest, Hungary.

[5]CNR - Istituto di Chimica Biomolecolare, Sezione Catania Via del Santuario 110, 95028 Valverde Catania, Italy.

* Corresponding author.

E-mail address: lpasquin@unict.it (Pasquinucci Lorella)

‡These authors share last authorship

Table of contents

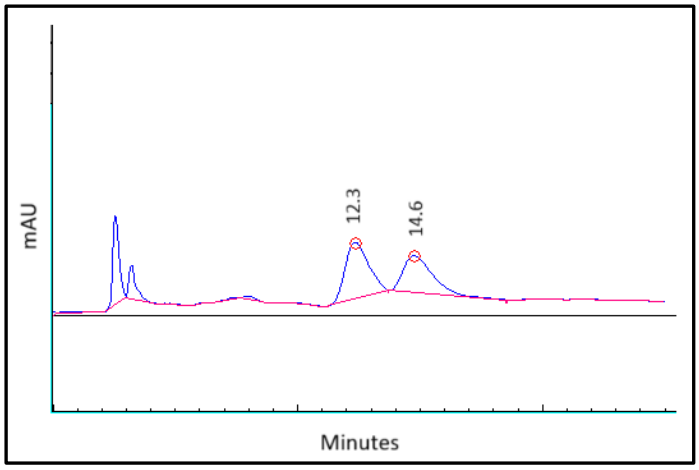

Figure S1. Chiral HPLC analysis of compound **7**. The composition of diastereomeric mixture was determined by chiral HPLC chromatography and carried out on a Varian system composed of a Varian 9010 pump and Varian 9050 variable wavelength UV-Vis detector. The chiral column was a Chiralcel OJ column from Daicel Chemical Industries (250 x 4.6 mm, 5 μm particle size). The analysis was performed with a mobile phase hexane-ethanol at 9:1 ratio, at 1.1 mL/min, an injection volume of 10 μL and the detector wavelength of λ=254 nm. The separation of diastereoisomeric mixture of compound **7** was showed with a peak at t_R = 12.3 min (55.6%) and a peak at t_R = 14.6 min (44.4%,), respectively.

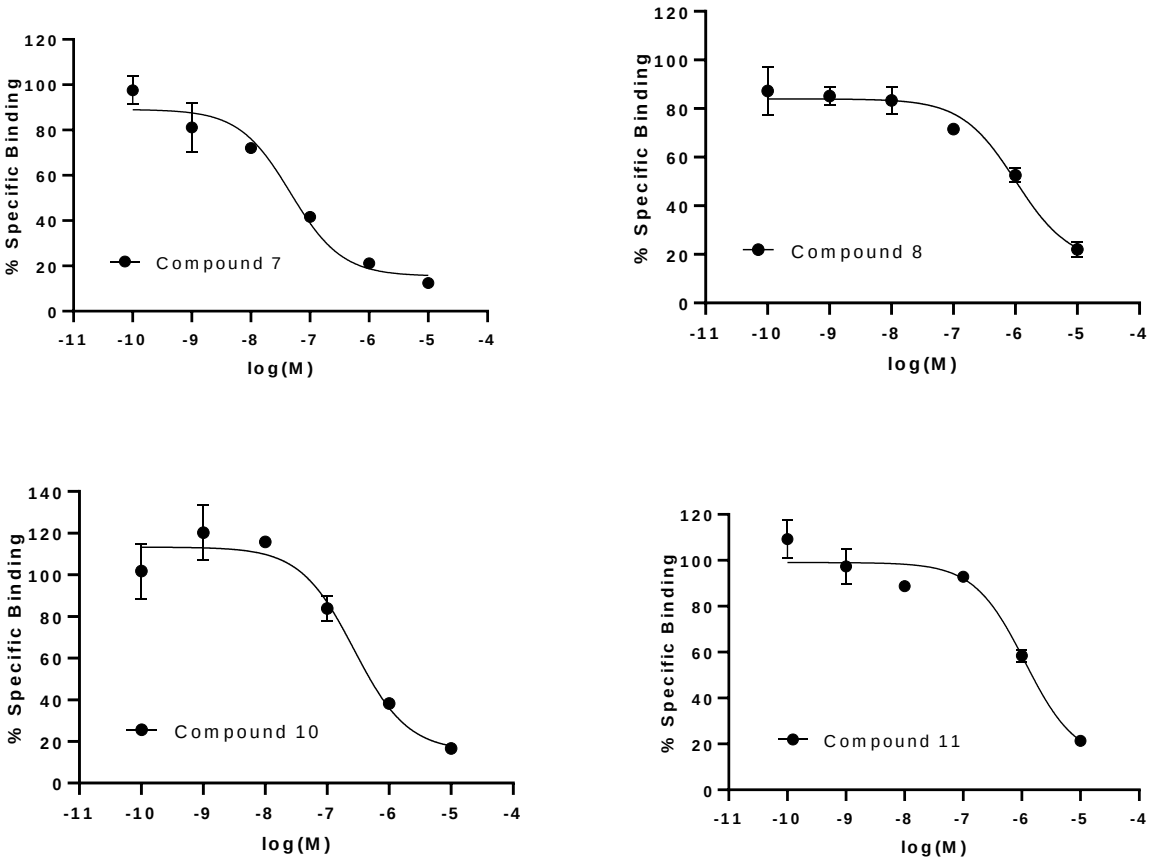

Figure S2. Competitive inhibition of [^{3}H]-(+)-pentazocine (2 nM) binding to guinea pig brain cortex membranes by unlabeled compounds **7**, **8**, and **10**–**11** at 10^{-10}–10^{-5} M concentration range. Data shown are expressed as percent-specific binding.

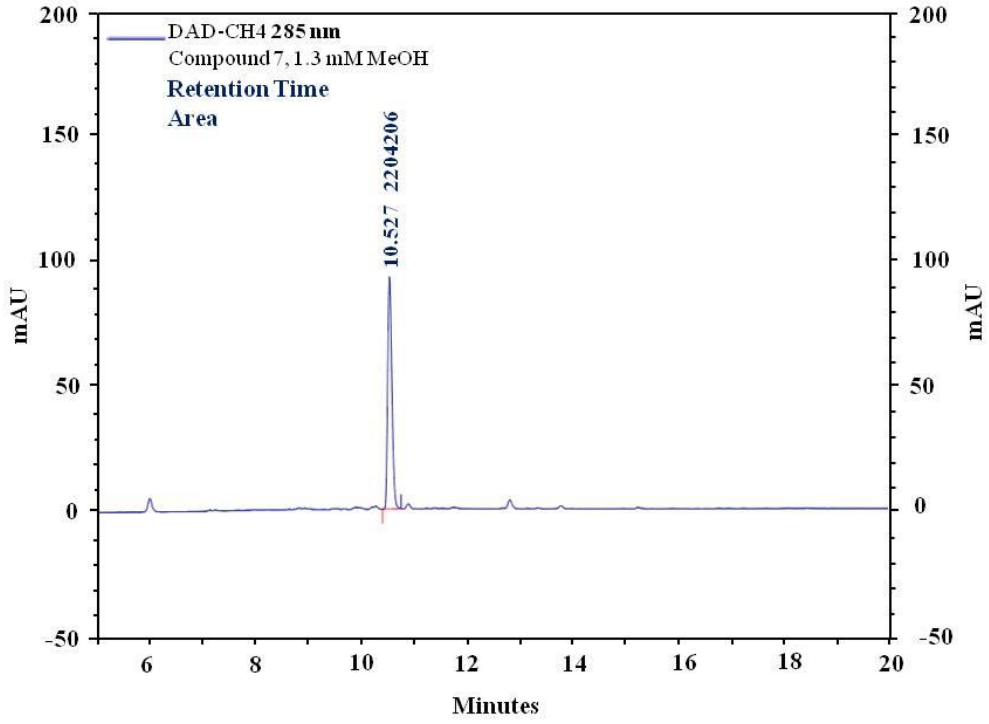

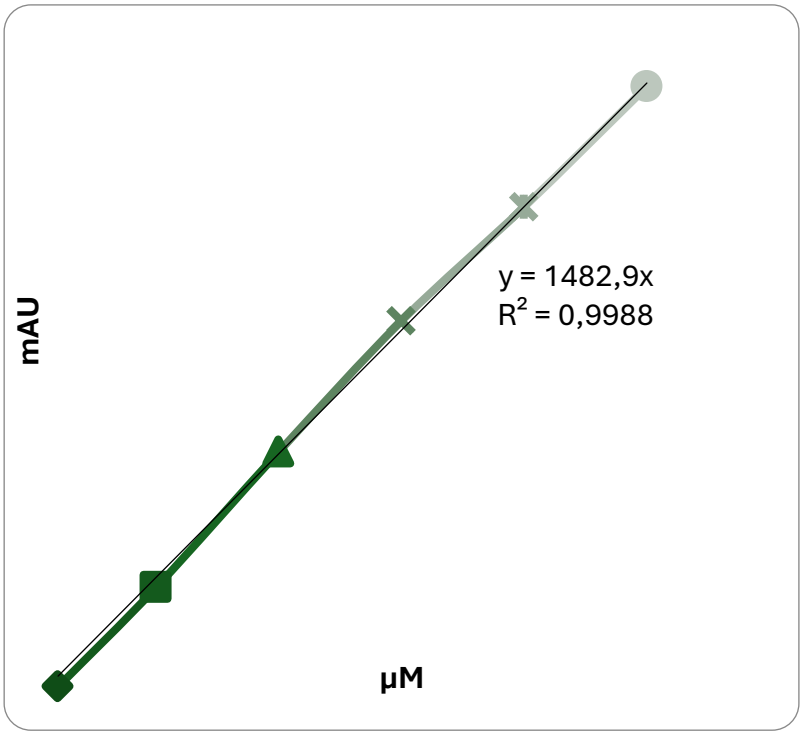

Figure S3. RP-HPLC analysis of compound **7**. Compound **7** (1.3 mM in methanol; injection volume, 10 µL) provided a sharp peak following RP-HPLC analysis, with an R_t of 10.52 min. A calibration curve of compound **7** was also performed as described in the *Experiment Section*, which gave a satisfactory linear regression model with a correlation coefficient (R^2) of 0.999 and a mathematical equation fit of y = 1482,9x.

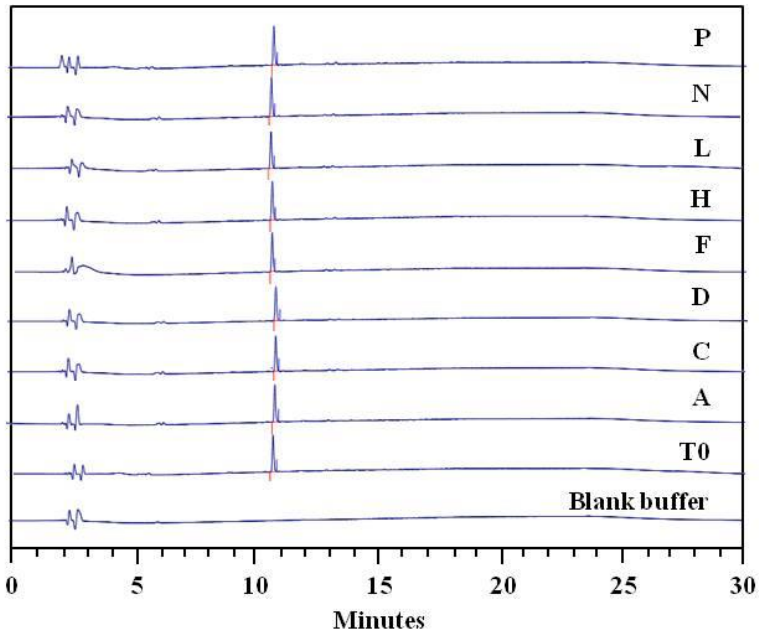

Buffer Solution λ= 285 nm	Compound **7** (mAU)
T0	213670
A	208635
C	203400
D	206888
F	218781
H	214584
L	214461
N	215881
P	220385

Figure S4. Stability in physiological phosphate buffer solution. Overlayed chromatograms of compound **7** in phosphate buffer solution (representative experiment). Test conditions included a blank, T_0, and 8 different incubation times with compound **7** and samples were analysed as described in the *Experiment Section*. At all incubation times, the levels of compound **7** remained constant, indicating its chemical stability up to 300 min under these conditions. Data in the table are expressed in mAU and reflect the mean of a single experiment with samples prepared and injected in duplicate. T0, time zero; A, 15 min; C, 30 min; D, 60 min; F, 90 min; H, 120 min; L, 180 min, N, 240 min; P, 300 min.

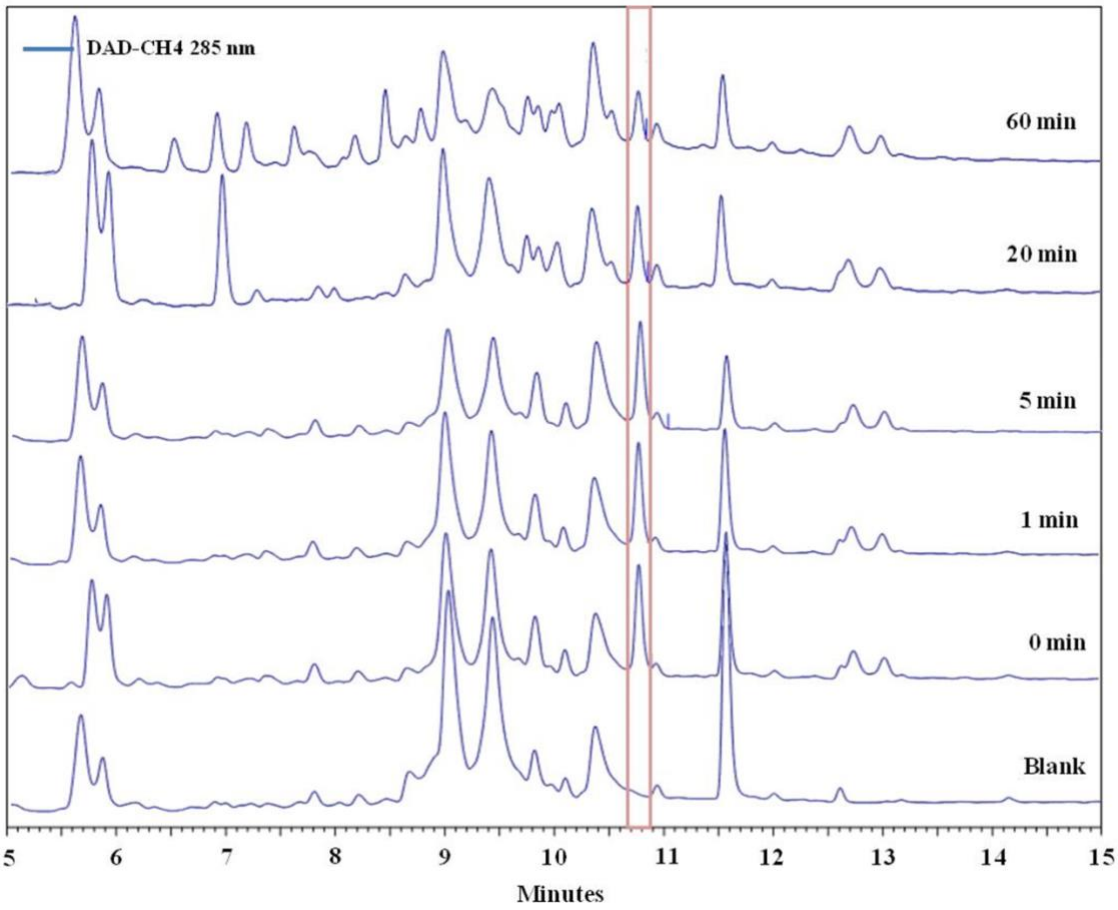

Figure S5. Overlayed chromatograms of compound **7** in rat plasma at different incubation times (0 to 60 min).

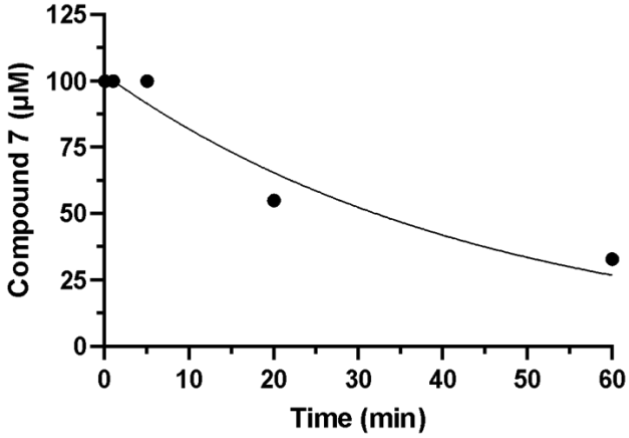

Figure S6. Estimation of the half-life (in min) of compound **7**, after different incubation times in rat plasma (from 0 to 60 min). Data were processed with GraphPad Prism 8.0 and provided a calculated half-life of 31.07 min.

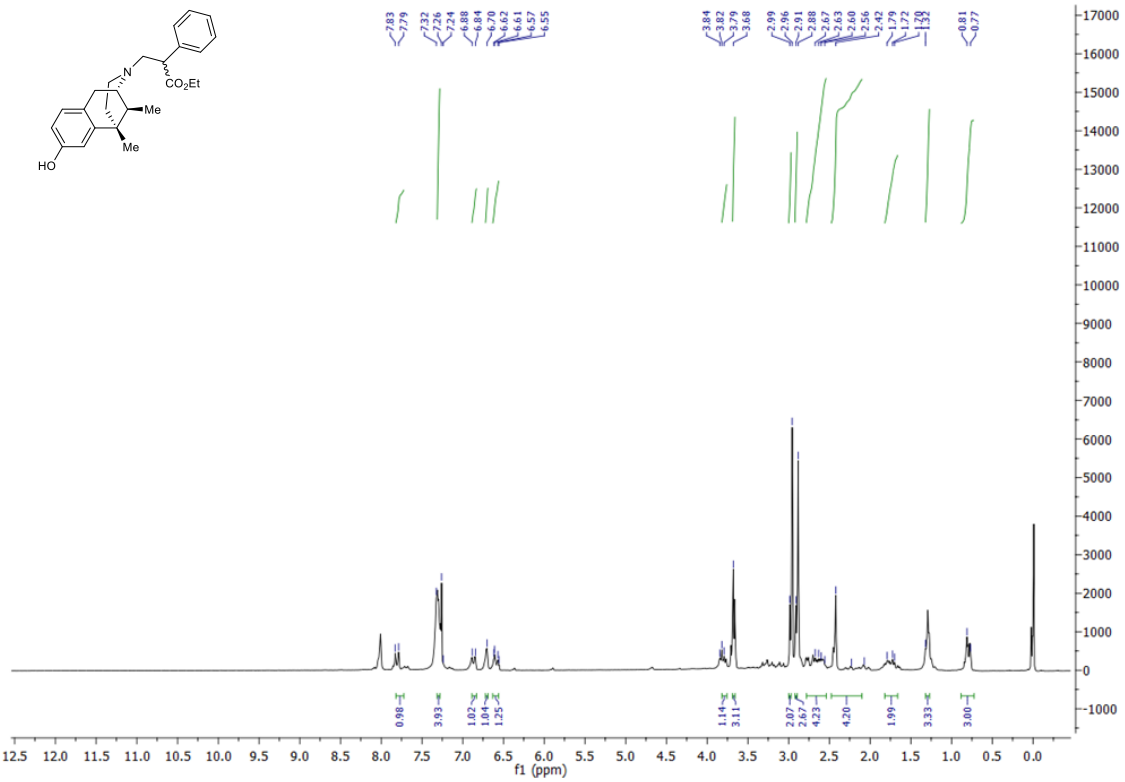

Figure S7. ^{1}H NMR spectrum of **6** in $CDCl_3$.

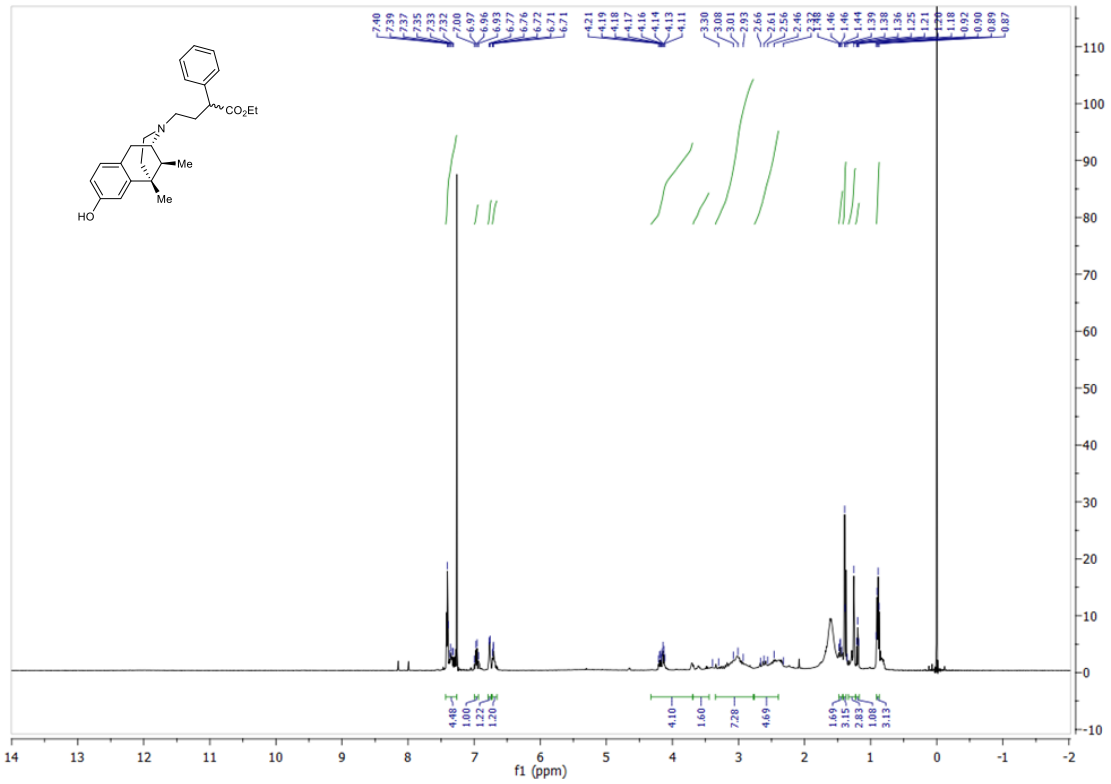

Figure S8. ^{1}H NMR spectrum of **7** in $CDCl_3$.

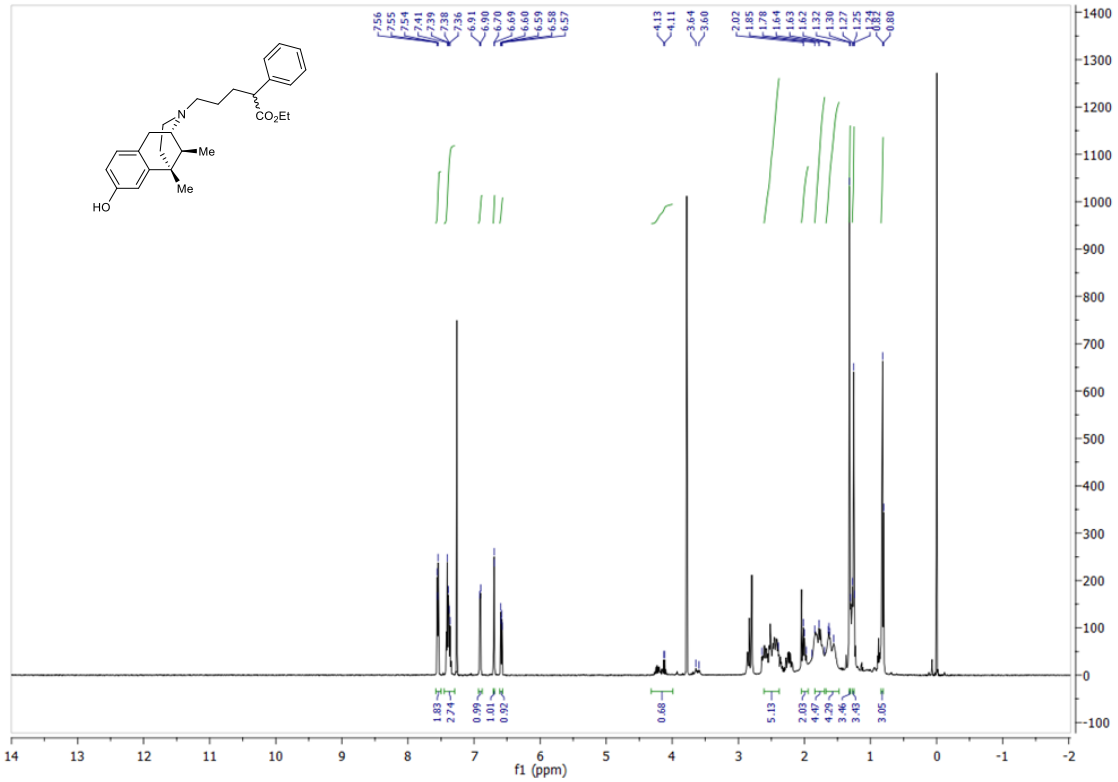

Figure S9. ^{1}H NMR spectrum of **8** in $CDCl_3$.

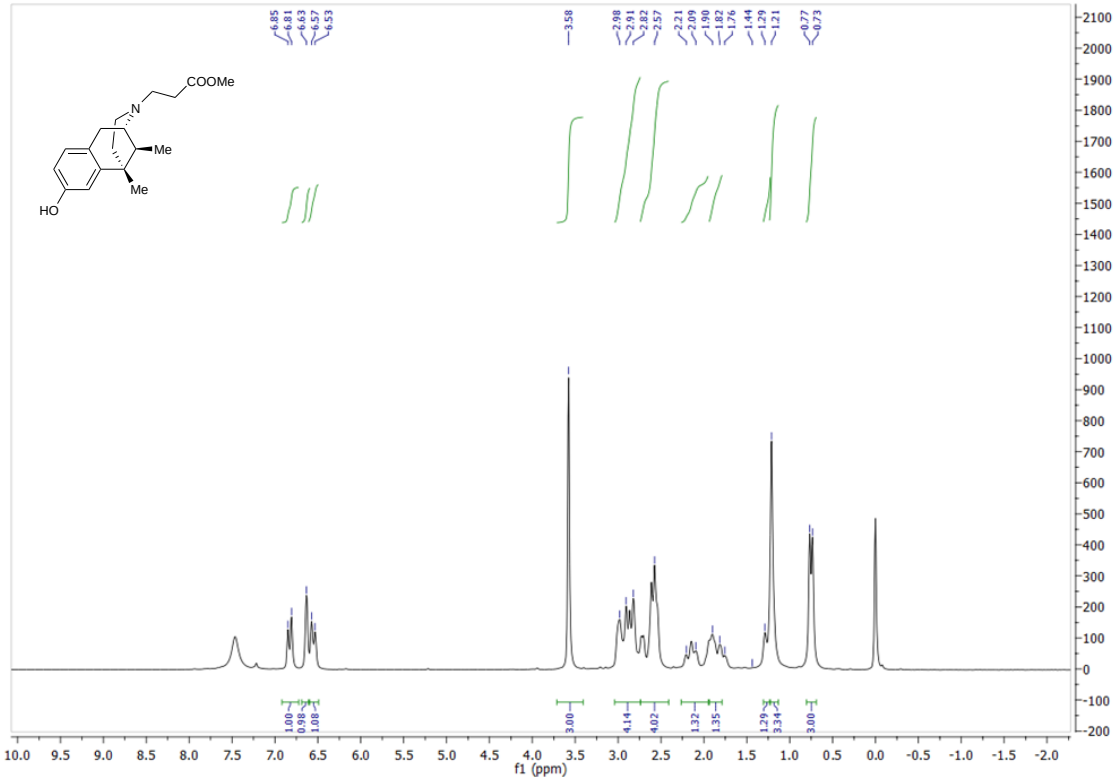

Figure S10. ^{1}H NMR spectrum of **9** in $CDCl_3$.

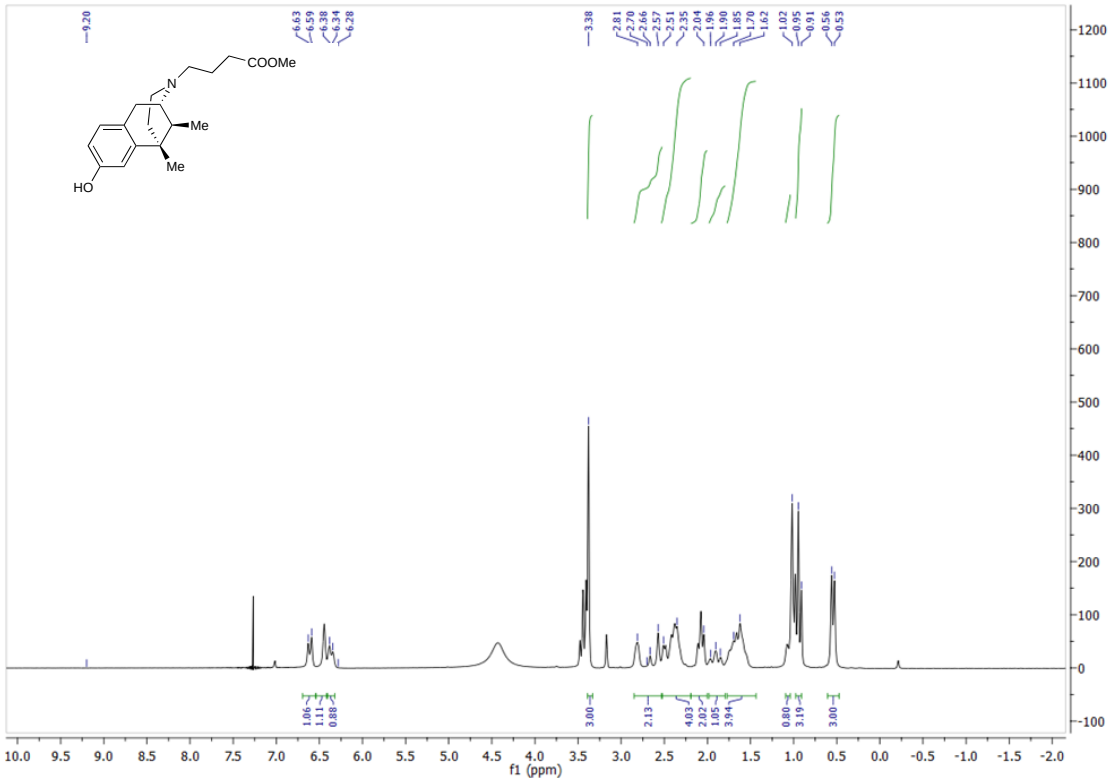

Figure S11. ^{1}H NMR spectrum of **10** in $CDCl_3$.

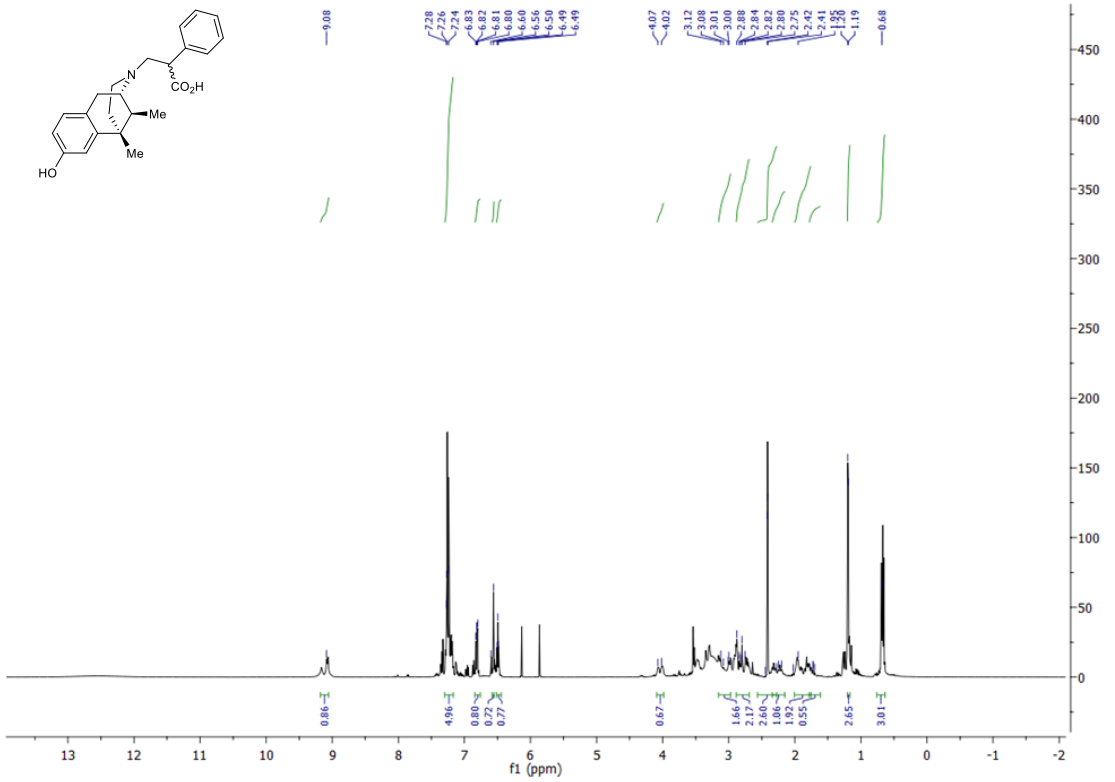

Figure S12. ^{1}H NMR spectrum of **11** in DMSO-d_6.

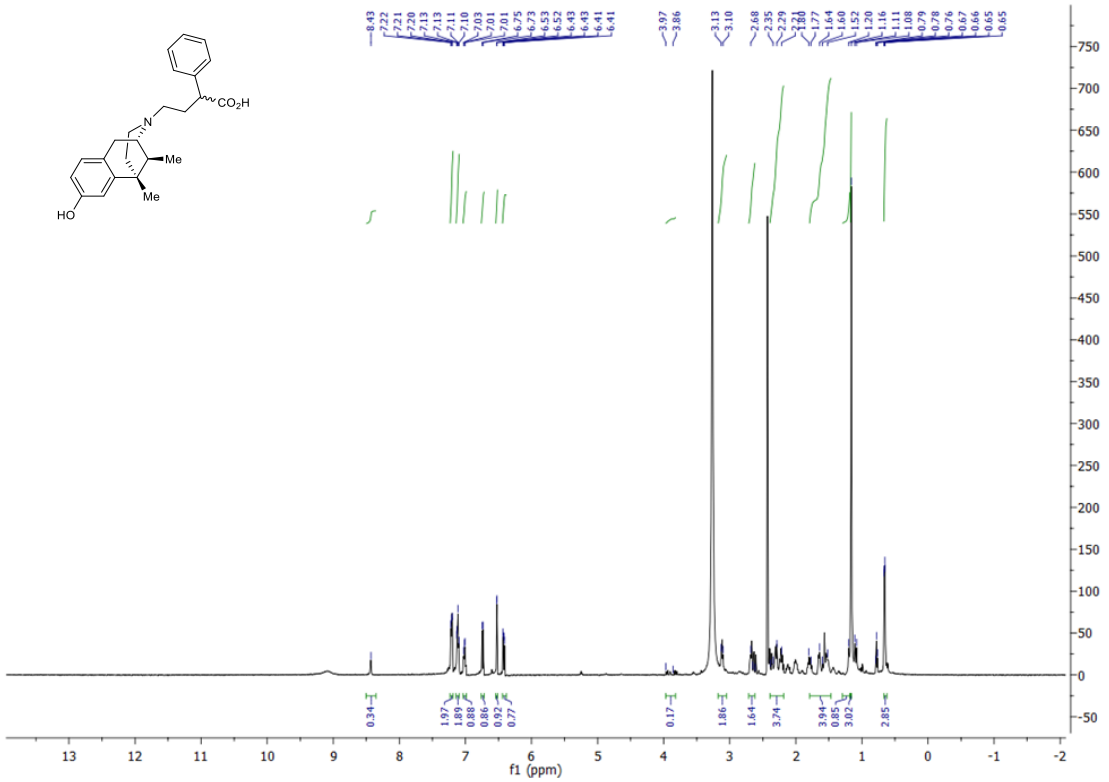

Figure S13. ^{1}H NMR spectrum of **12** in DMSO-d_6.

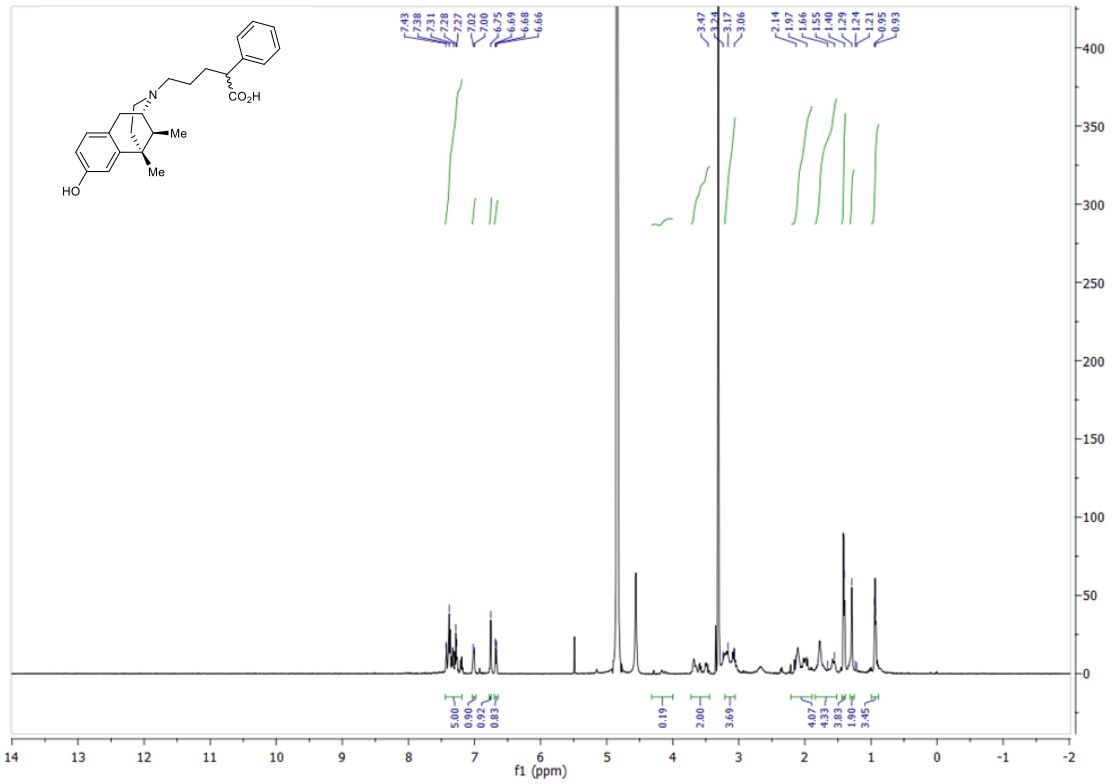

Figure S14. ^{1}H NMR spectrum of **13** in DMSO-d_6.

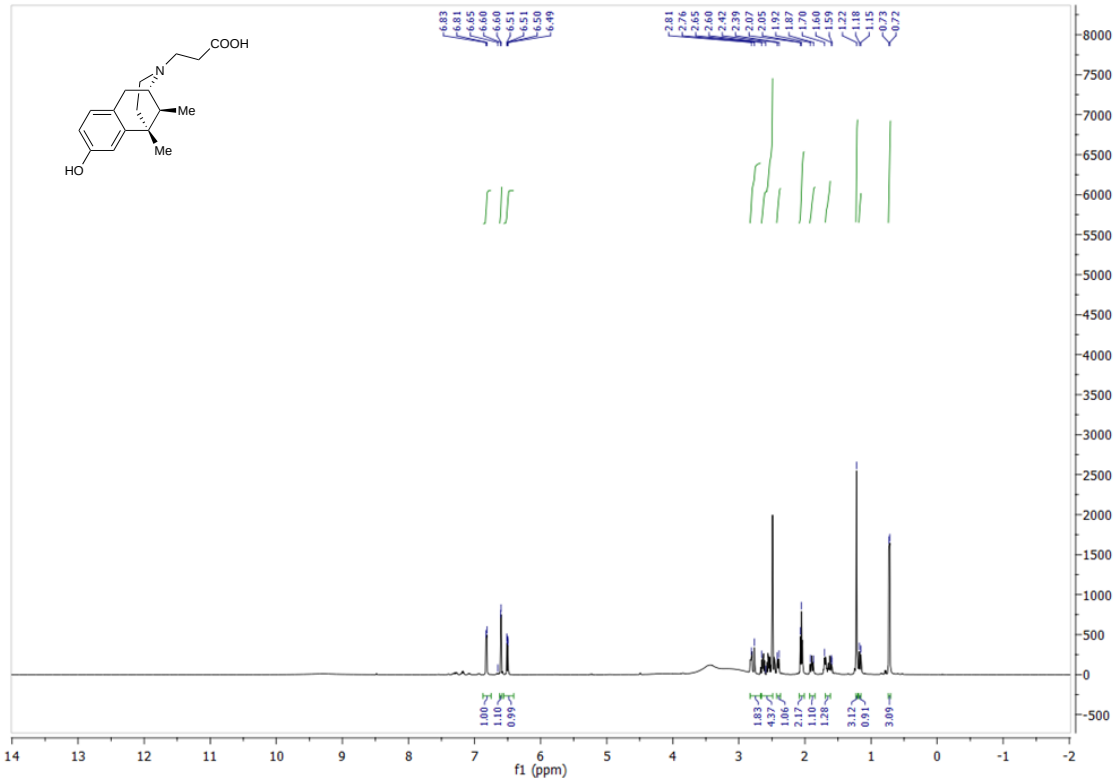

Figure S15. ^{1}H NMR spectrum of **14** in DMSO-d_6.

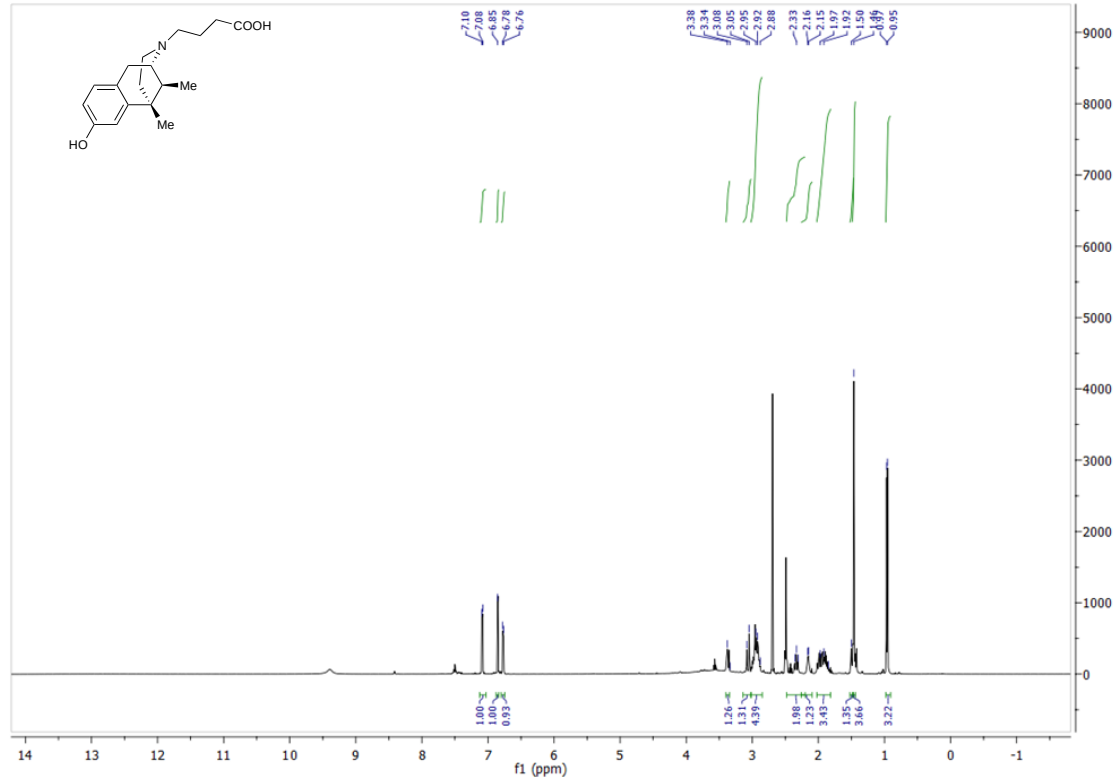

Figure S16. ^{1}H NMR spectrum of **15** in DMSO-d_6.

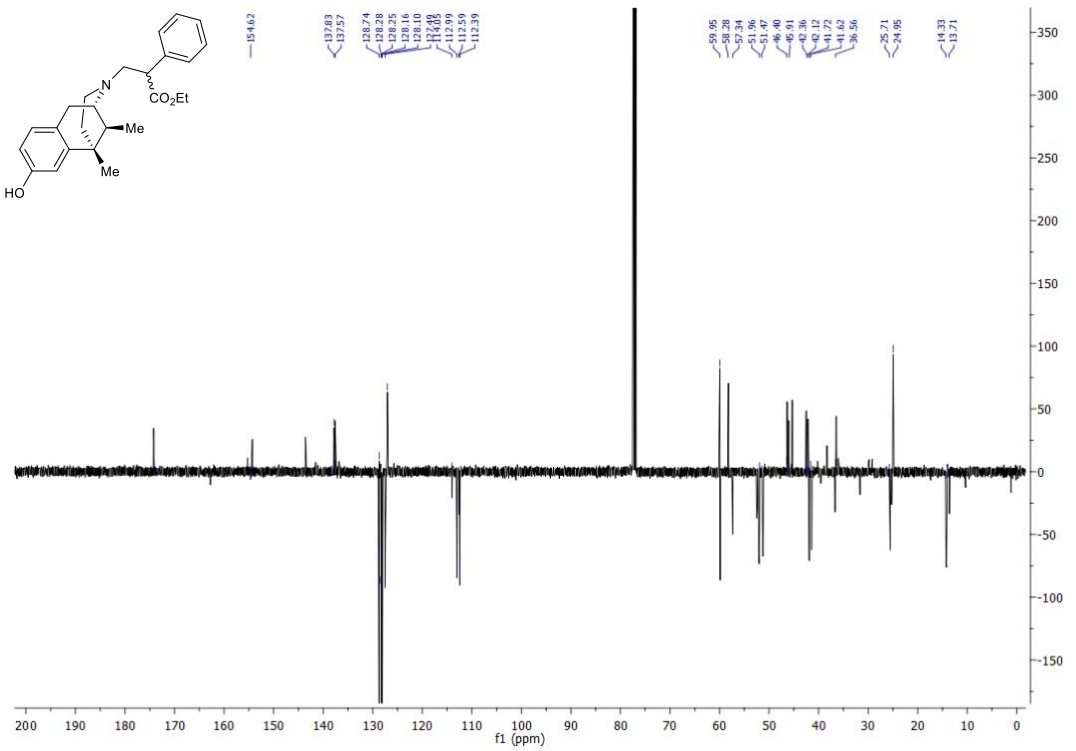

Figure S17. APT NMR spectrum of **6** in $CDCl_3$

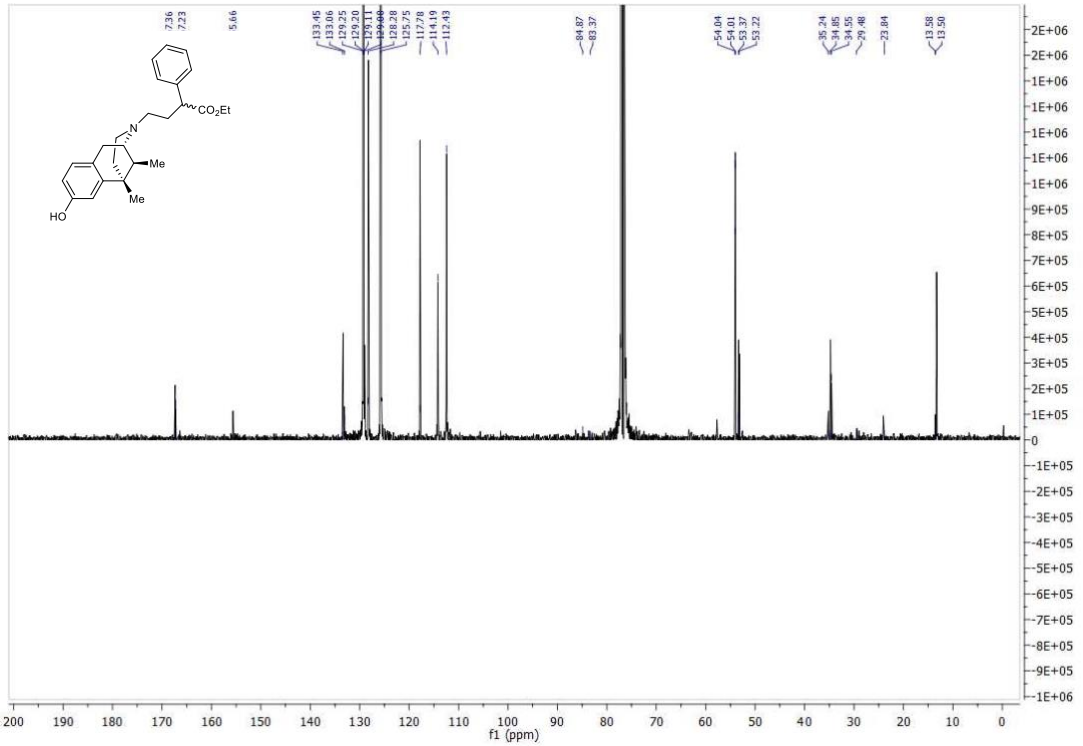

Figure S18. ^{13}C NMR spectrum of **7** in $CDCl_3$

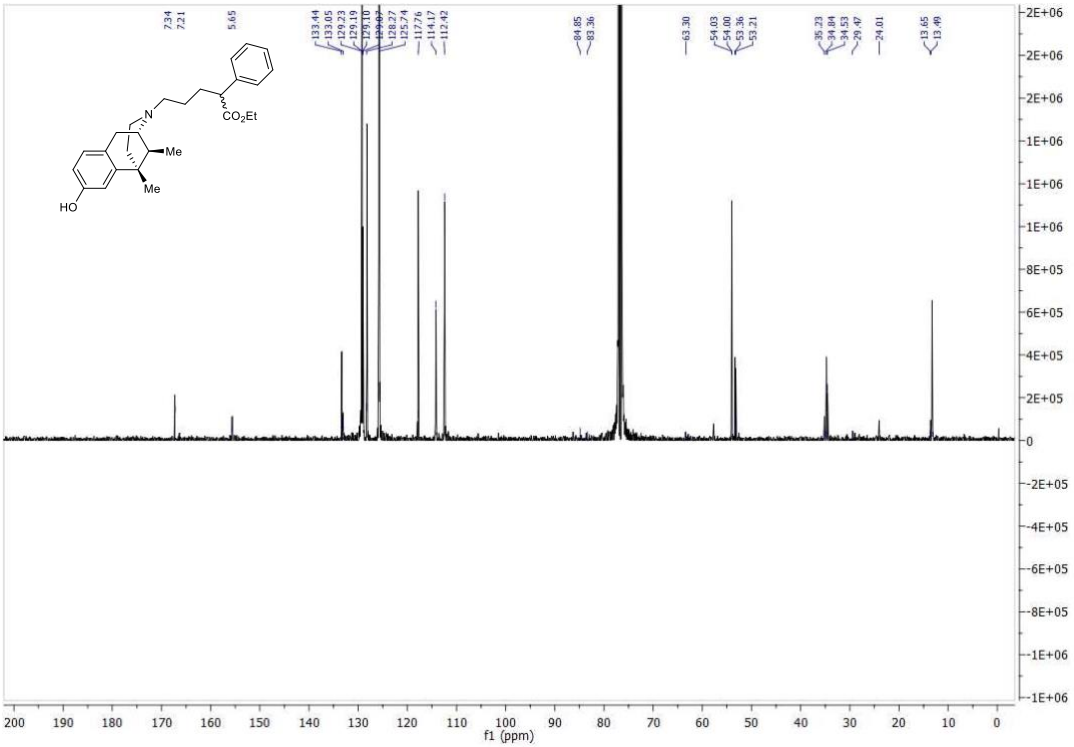

Figure S19. ^{13}C NMR spectrum of **8** in $CDCl_3$.

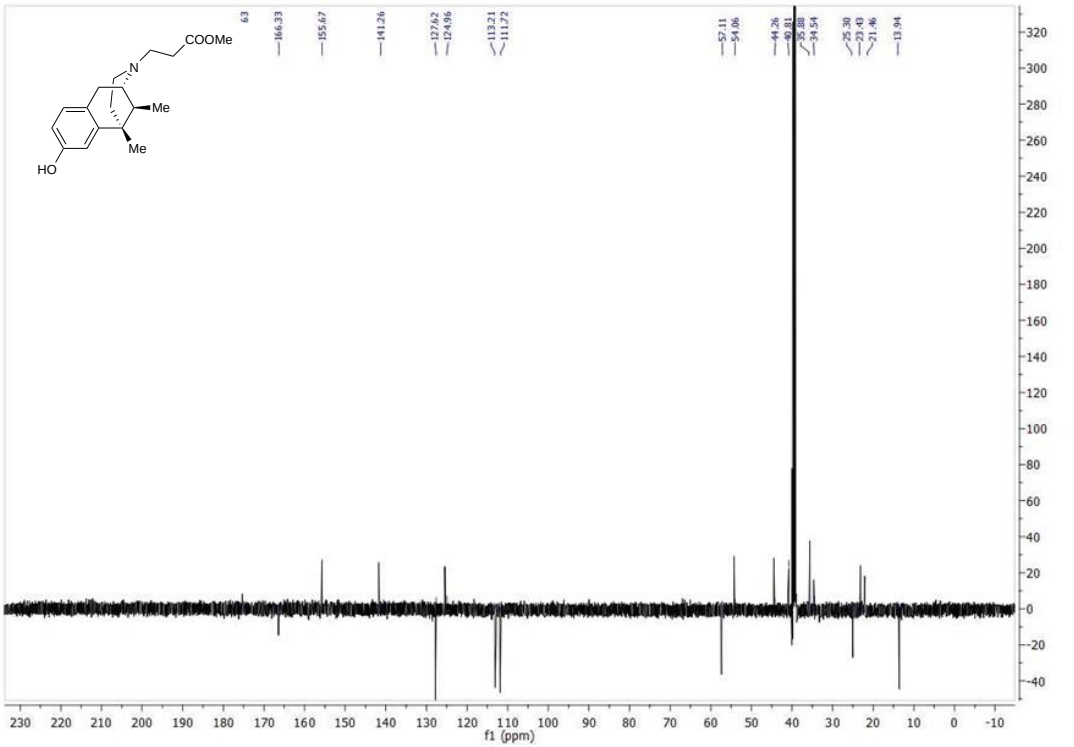

Figure S20. APT NMR spectrum of **9** in DMSO-d_6.

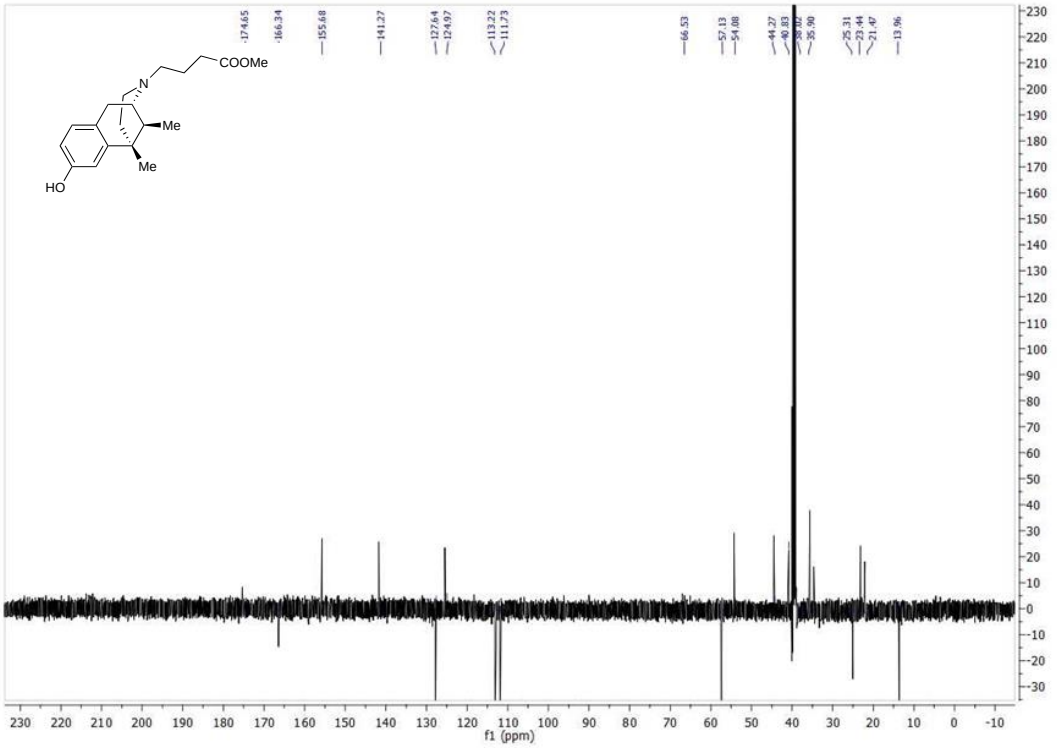

Figure S21. APT NMR spectrum of **10** in DMSO-d_6.

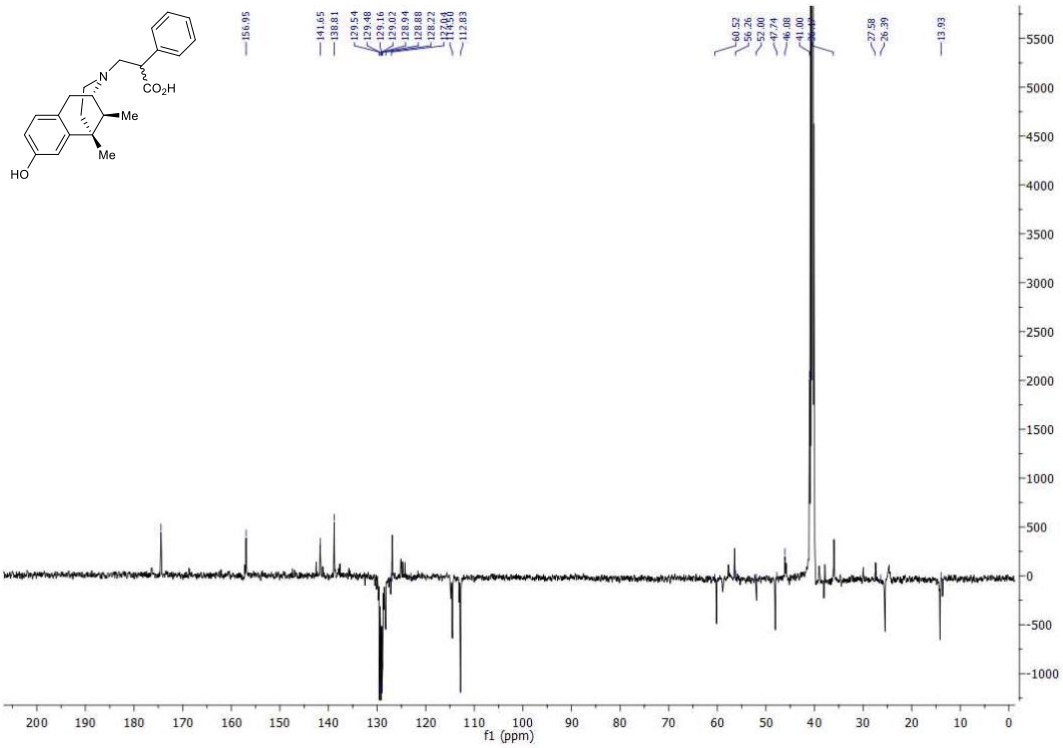

Figure S22. Figure S21. APT NMR spectrum of **11** in DMSO-d_6.

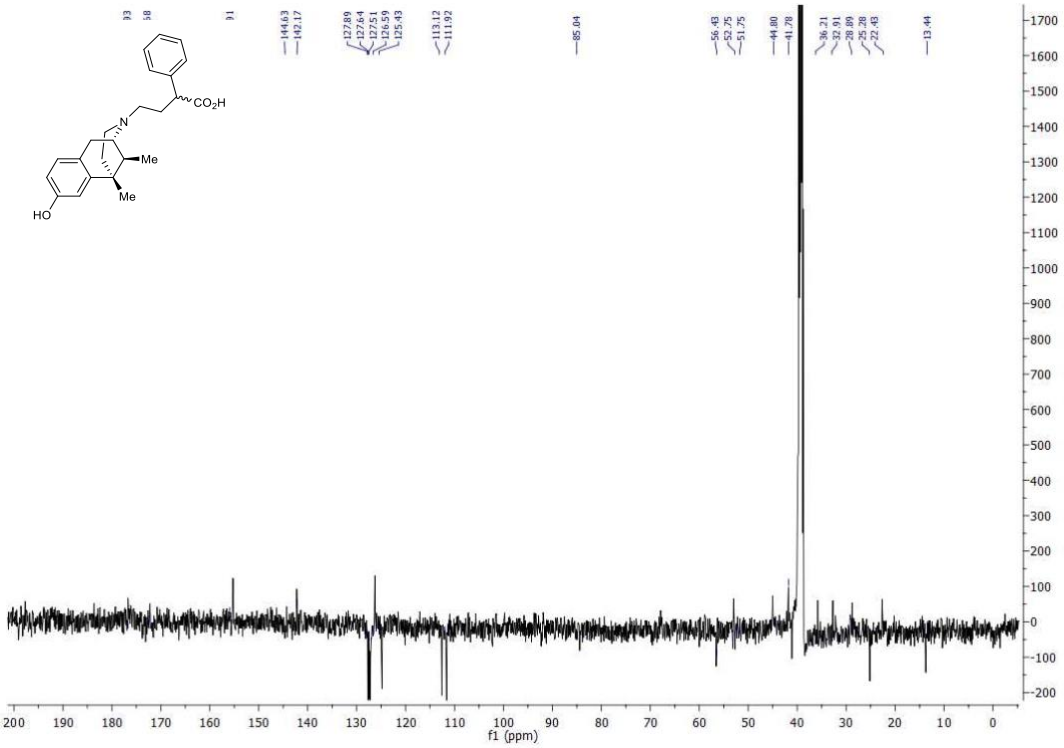

Figure S23. APT NMR spectrum of **12** in DMSO-d_6.

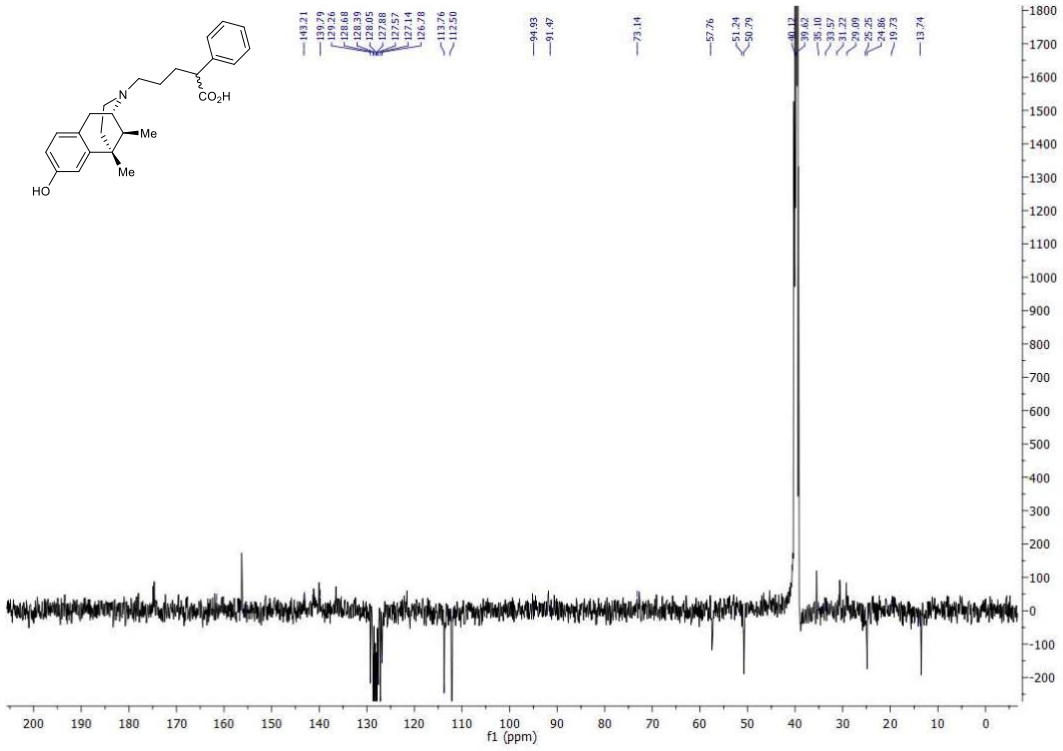

Figure S24. APT NMR spectrum of **13** in DMSO-d_6.

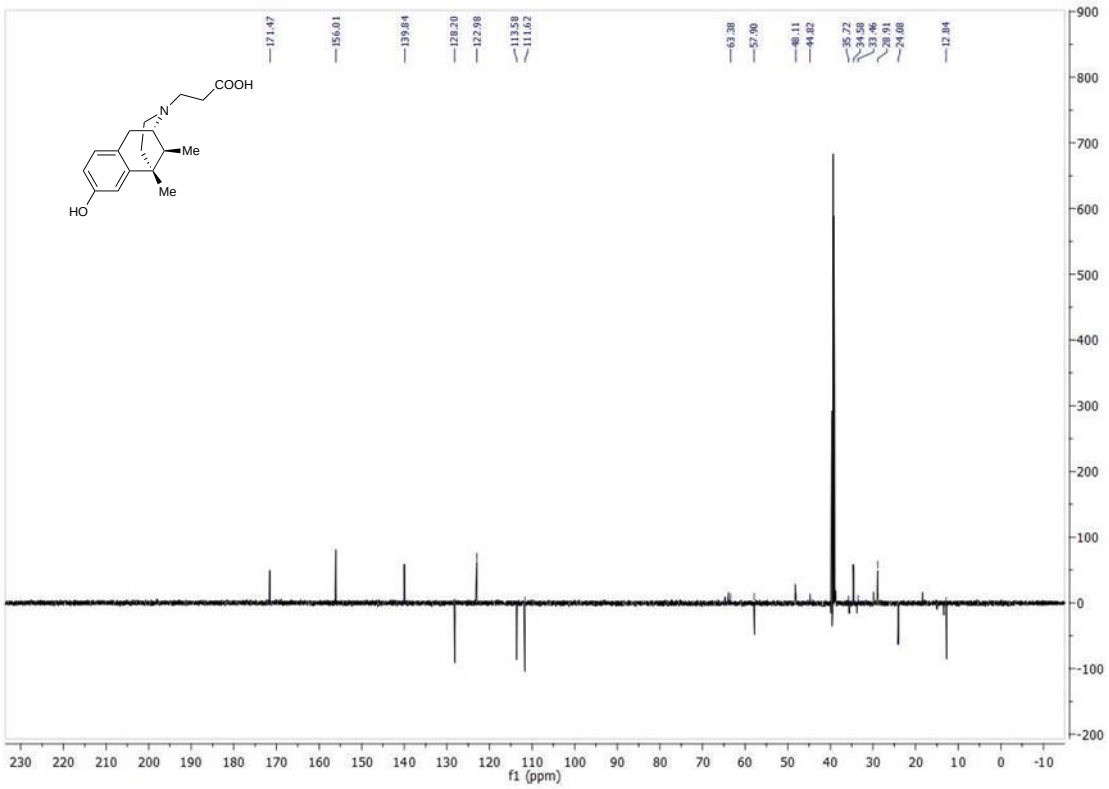

Figure S25. APT NMR spectrum of **14** in DMSO-d_6.

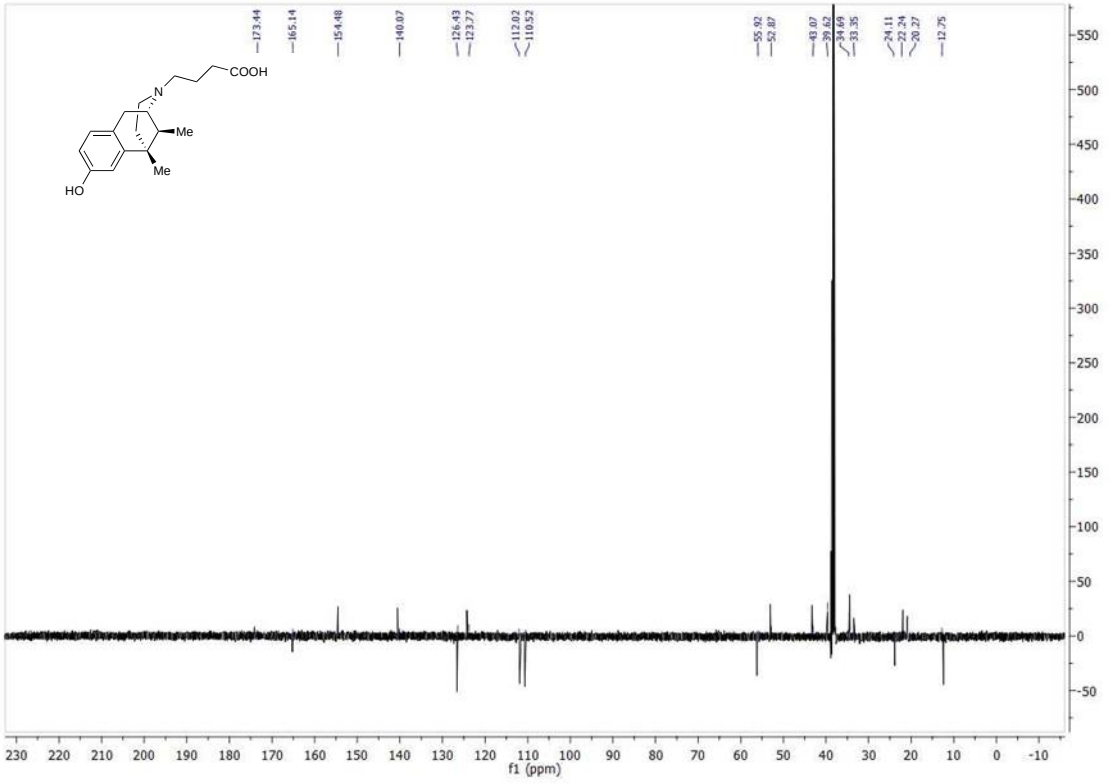

Figure S26. APT NMR spectrum of **15** in DMSO-d_6.

Table S1. Elemental analysis data for compounds **6**−**15**.

			Calcd			Found		
Compd	**Formula**	**MW**	**C**	**H**	**N**	**C**	**H**	**N**
6	$C_{25}H_{31}NO_3$	393.53	76.30	7.94	3.56	76.40	7.90	3.55
7	$C_{26}H_{33}NO_3$	407.55	76.62	8.16	3.44	76.67	8.15	3.46
8	$C_{27}H_{35}NO_3$	421.57	76.92	8.37	3.32	76.95	8.33	3.35
9	$C_{18}H_{25}NO_3$	303.40	71.26	8.31	4.62	71.23	8.34	4.63
10	$C_{19}H_{27}NO_3$	317.43	71.89	8.57	4.41	71.91	8.59	4.40
11	$C_{23}H_{27}NO_3$	365.47	75.59	7.45	3.83	75.63	7.43	3.85
12	$C_{24}H_{29}NO_3$	379.49	75.96	7.70	3.69	76.95	7.75	3.59
13	$C_{25}H_{31}NO_3$	393.52	76.30	7.94	3.56	76.27	7.80	3.55
14	$C_{17}H_{23}NO_3$	289.37	70.56	8.01	4.84	70.53	8.03	4.86
15	$C_{18}H_{25}NO_3$	303.40	71.26	8.31	4.62	71.27	8.30	4.63